Time Versus Frequency Domain full Waveform Inversion for Ultrasound Imaging

Ramirez, Ana B.; Abreo, Sergio A.; Van Dongen, K. W.A.

DOI
10.1109/IUS54386.2022.9958916

Publication date
2022

Document Version
Final published version

Published in
IUS 2022 - IEEE International Ultrasonics Symposium

Time Versus Frequency Domain full Waveform Inversion for Ultrasound Imaging

Ana B. Ramirez
Electrical and Electronics Depart.
Universidad Industrial de Santander
Bucaramanga, Colombia
anaberam@uis.edu.co

Sergio A. Abreo
Electrical and Electronics Depart.
Universidad Industrial de Santander
Bucaramanga, Colombia
0000-0001-7094-4734

K.W.A. van Dongen
Dept. of Imaging Physics
Delft University of Technology
Delft, The Netherlands
K.W.A.vanDongen@tudelft.nl

***Abstract*—With full waveform inversion (FWI) all available information enclosed in the recorded wavefield – including multiple scattering, dispersion, and diffraction – is used to obtain accurate images showing quantitative information of the tissue parameters. These non-linear inversion methods are implemented either in the time or in the frequency domain. Unfortunately, selecting which implementation should be used for a specific problem is not trivial. To ease the selection process, we compare the performance of one time-domain inversion (TDI) and one frequency-domain inversion (FDI) - also known as Contrast Source Inversion - to provide insights into the strengths and weaknesses of each FWI method. In this contribution, we investigate the effect of the (i) bandwidth, (ii) problem complexity, (iii) number of sources and receivers, and (iv) initial speed-of-sound model on the performance of each FWI method by comparing the resulting reconstructions. Both methods are tested for the same configuration: a 2-D tomographic scan of a cancerous breast model. To avoid an inverse crime, TDI is tested on synthetic data obtained using a frequency-domain forward solver and CSI on data from a time-domain forward solver.**

***Index Terms*—Time-domain inversion, frequency-domain inversion, ultrasound imaging, full waveform inversion**

I. Introduction

Ultrasound imaging is a medical imaging modality that uses high-frequency sound waves to produce images from inside the body. Particularly, ultrasound imaging is considered a diagnostic or screening procedure for breast cancer detection [1], [2]. Ultrasound imaging uses different reconstruction methods such as time-of-flight tomography (TOFT), Born inversion (BI) or synthetic aperture focusing technique (SAFT) to obtain an image of the echogenicity of the breast. Modern reconstruction methods use the entire information of the transducer to obtain quantitative images of the tissues inside the breast [3]. These methods are referred as full waveform inversion (FWI) methods. Although FWI was originally developed in geophysics, different FWI methods, in both time and frequency, have been also been applied in ultrasound imaging [5] - [7]. A review of different imaging and inversion methods for medical ultrasound tomography can be found here [4].

In this work, we compare time and frequency domain FWI for ultrasound imaging in terms of (i) bandwidth, (ii) problem complexity, (iii) number of sources and receivers, and (iv) initial speed-of-sound model. Advantages and disadvantages of both methods, time or frequency FWI, are presented here to give insights on which method is more suitable depending on the application.

II. Methods

A. Time Domain Inversion

The time domain wave equation is given by

$$\nabla^2 p_j(x,t) - \frac{1}{c^2(x)}\frac{\partial^2 p(x,t)}{\partial t^2} = -S_j(x,t), \tag{1}$$

where $c(x)$ is the velocity profile of the breast, t is the time variable and $S_j(x,t)$ is the jth primary source generating the wave field. The inverse problem consist on estimating $c(x)$ from the wave field measured at the receivers location. The reconstruction of the velocity profile can be set as follows

$$\min_{c(x)} \|p_j^{mod} - p_j^{obs}\|_{S_2}^2, \tag{2}$$

where $\|\cdot\|_{S_2}^2$ is the ℓ_2-norm in the data domain. The solution of the problem in (2) can be obtained iteratively using a Gauss-Newton method. The reconstructed velocity profile is given by

$$c^k = c^{k-1} - \alpha \cdot H^{-1}(c^{k-1}) \cdot g(c^{k-1}), \tag{3}$$

where $H^{-1}(c^{k-1})$ is the inverse of the Hessian matrix and $g(c^{k-1})$ is the gradient of the cost function. Since computing the Hessian matrix is very expensive computationally, the LBFGS algorithm is used to compute an approximation of the Hessian matrix.

B. Frequency Domain Inversion

In the frequency domain, with angular frequency ω, the wave field can be described by a summation of two wave fields as follows

$$p_j(x,\omega) = p_j^{inc}(x,\omega) + p_j^{sct}(x,\omega), \tag{4}$$

where $p_j^{inc}(x,\omega)$ is the incident field generated by the source $S_j(x,\omega)$ and propagating in the homogeneous background medium with speed of sound c_0, and $p_j^{sct}(x,\omega)$ is the scattered field. The frequency domain equation can be written as the

2022 IEEE International Ultrasonics Symposium (IUS) | 978-1-6654-6657-8/22/$31.00 ©2022 IEEE | DOI: 10.1109/IUS54386.2022.9958916

following in-homogeneous Fredholm integral equation of the second kind

$$p_j(x,\omega) = p_j^{inc}(x,\omega) + \int_{x'\in D} G(x-x',\omega)w_j(x',\omega)dA(x'), \quad (5)$$

where $G(x-x',\omega)$ is the Green's function and $w_j(x,\omega)$ is an unknown contrast source function given by

$$w_j(x',\omega) = \chi(x')p_j(x',\omega), \quad (6)$$

in which $\chi(x')$ is the contrast function.
Given the measured wave field, the unknown contrast source term w_j is estimated using an iterative scheme, which minimizes the following cost function

$$\min_{w_j} \eta_S \|p_j^{sct} - L^S[w_j]\|_{S_2}^2 + \eta_D\|\chi p_j^{inc} - w_j + \chi L^D[w_j]\|_{D_2}^2, \quad (7)$$

where $\|\cdot\|_{S_2}^2$ and $\|\cdot\|_{D_2}^2$ represent the ℓ_2-norm in the data and object domain, respectively; and η_S and η_D are normalization terms. From the updated contrast source w_j, the unknown total field p_j inside the object domain is also updated and, finally, the contrast function is obtained by

$$\chi = \frac{\Re\{<p_j, w_j>_D\}}{\|p_j\|_{D_2}^2}. \quad (8)$$

Finally, the speed-of-sound profile is computed from the contrast function as

$$c = \frac{1}{\sqrt{\chi + c_0^{-2}}}. \quad (9)$$

III. Results

In order to compare the performance of time domain inversion (TDI), and frequency domain inversion (FDI), both methods are tested using the configuration in Figure 1, a breast with a cancerous tumor enclosed by a circular array of transducers. The employed breast model is derived from a MRI scan of a cancerous breast [8]. The circular array has a diameter of 259mm. The four types of tissue in the breast model are: glandular tissue ($c = 1540\text{m/s}$), tumor ($c = 1572\text{m/s}$), skin ($c = 1577\text{m/s}$), and fat ($c = 1437\text{m/s}$). The breast is submerged in water ($c_0 = 1520\text{m/s}$). Depending on the acquisition setup, the array contains 30, 150 or 157 transducers. Each transducer can act as a source to generate a Gaussian modulated wave field with a center frequency $f_0 \approx 90\text{KHz}$. Finally, the spatial domain contains 128×128 elements of size $\Delta x \times \Delta y \approx 2.2 \times 2.2\text{mm}$ For the TDI method, a temporal step size $\Delta t = 0.33$ μs is used resulting in $N_t = 1600$ time samples; and for the FDI method, a temporal step size $\Delta t = 2.76$ μs resulting in $N_t = 200$ time samples.

A. Bandwidth

First, both TDI and FDI are evaluated in the reconstruction of the speed-of-sound profile depending on the bandwidth used during the inversion. In all experiments, the number of sources and receivers are $N_s = 157$ and $N_r = 157$. Figure 2 shows the reconstruction when full bandwidth is used in time and

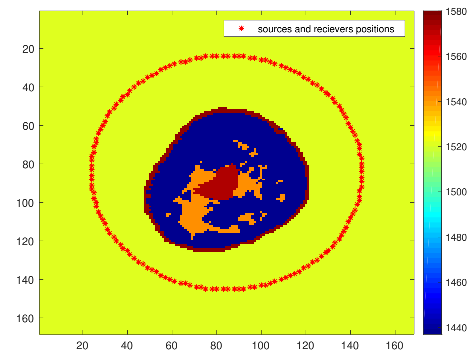

Fig. 1. Breast model. Configuration of the circular array of sources and receivers.

frequency domain. Also, the reconstruction of the speed-of-sound profile is tested when only a set of 30 frequencies is used during the inversion. For the time domain inversion, the scans are filtered using a sharp filter in frequency. Note, in Fig. 2 that the reconstruction for TDI and FDI using full bandwidth is similar. But, on the other hand, when limited bandwidth is used, TDI does not converge to a correct solution. This result can be explained by the fact that when the time-domain scans are filtered with a very selective filter, many signal oscillations are generated and the TDI suffers of cycle-skipping.

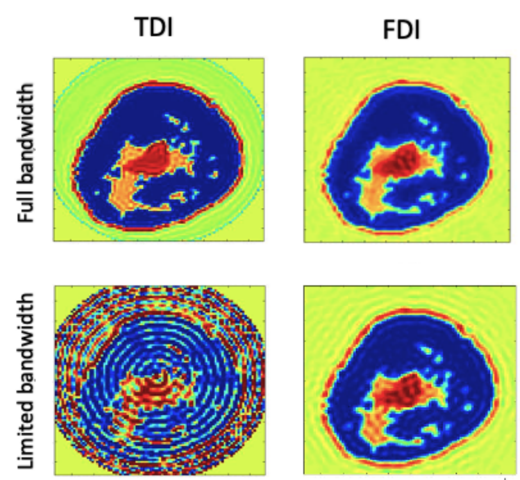

Fig. 2. Reconstruction of the speed-of-sound profile for full and limited bandwidth.

B. Problem Complexity

Table I presents the complexity of each problem: TDI and FDI, in terms of the number of observations N_{obs} and number of unknowns N_{unk}. The problem formulated in the frequency domain has larger number of unknowns than the one formulated in the time domain. Besides, both methods have the same number of observations, when the number of time samples and frequency samples are the same. Note that in TDI, when the number of sources and receivers is large

TABLE I
PROBLEM COMPLEXITY FOR TDI AND FDI.

Method	Problem Complexity
TDI	$N_{obs} = N_s \times N_r \times N_t$ $N_{unk} = N_x \times N_y$
FDI	$N_{obs} = N_s \times N_r \times N_f$ $N_{unk} = N_s \times N_x \times N_y \times N_f$

TABLE II
MEMORY REQUIREMENTS FOR TDI AND FDI.

Method	Memory Requirements
TDI	$4 \cdot N_t \cdot N_s \cdot (N_x + 2N_{PML}) \cdot (N_y + 2N_{PML})$
FDI	$16 \cdot N_f \cdot N_s \cdot N_x \cdot N_y$

enough then $N_{obs} > N_{unk}$, and the problem is determined or over-determined. On the other hand, in FDI, the problem is always under-determined, i.e. $N_{obs} < N_{unk}$.

Also, the memory requirements of both FWI methods are presented in Table II. Note that in Table II the amount of memory required by TDI is larger than the memory required by FDI, as $N_t > N_f$. The number of time samples are chosen to satisfy the Courant's condition in the finite-differences discretization. For the experiment setup presented in this work, for instance, $N_t > 8N_f$.

C. Acquisition Setup

Now, TDI and FDI are evaluated in the reconstruction of the speed-of-sound profile for a set of different number of sources and receivers during the inversion. The number of sources and receivers are equally distributed around the circle. Three different experiments are tested: (i) $N_s \times N_r = 30 \times 30$, (ii) $N_s \times N_r = 6 \times 150$, (iii) $N_s \times N_r = 150 \times 6$ and (iv) $N_s \times N_r = 157 \times 157$. Figure 3 depicts the reconstruction for all the experiments for TDI and FDI. Note in Figure 3 that, for low number of sources and receivers, the performance of TDI is better than the performance of FDI, which can be explained by the complexity of the problem in the frequency domain. Also, in the frequency domain, the number of receivers is important, as the number of observations increases as the number of receivers also increases, whereas the number of sources is not relevant because as the number of sources increases, both the number of observations and the number of unknowns increases. For the case of full sources and receivers, the reconstruction for both time and frequency are similar. A good starting model (having enough low-frequency content) is also required for both methods to guarantee convergence if the number of sources and receivers is low.

D. Initial Speed-of-Sound Profile

As the problem formulation can be under-determined due to the lack of sources and receivers, the starting model is crucial for a correct reconstruction of the speed-of-sound profile. Also, a good starting model can avoid cycle-skipping problems. Figure 4 shows the reconstruction of the profile for

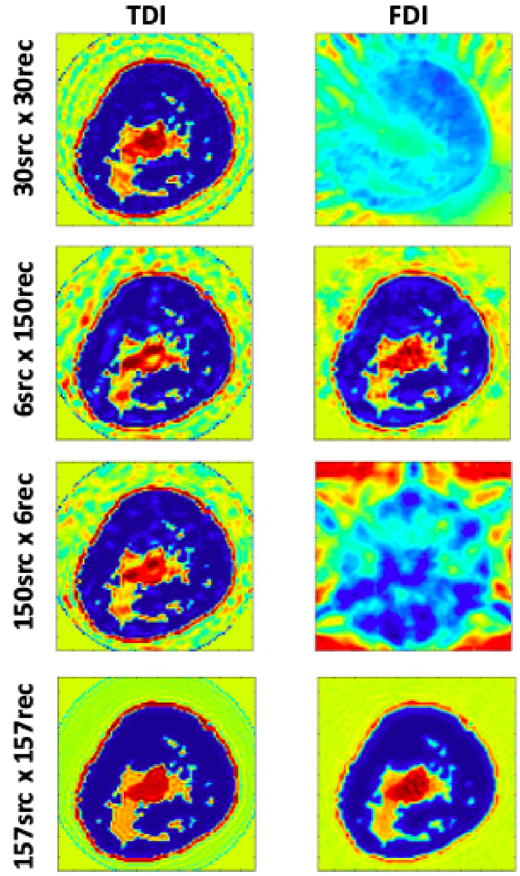

Fig. 3. Reconstruction of the speed-of-sound profile for different configuration of sources and receivers.

both TDI and FDI when the starting model is water or is a low-frequency reconstruction model, for full sources and receivers setup. Note in Fig. 4 that starting from a low-frequency model gives a better final reconstruction in FDI when only one frequency is used in the inversion, whereas that the solution for TDI is similar.

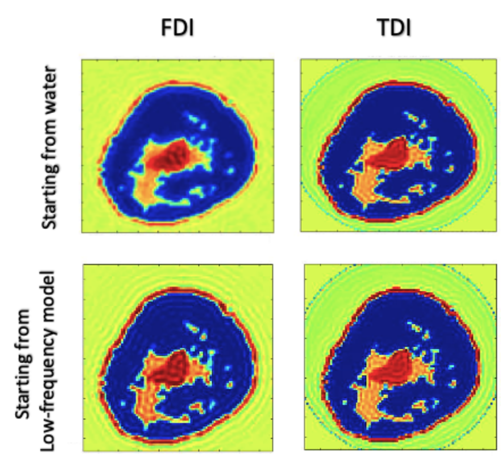

Fig. 4. Reconstruction of the speed-of-sound profile starting from a water model and a low-frequency model.

IV. Conclusions

In general, TDI slightly outperforms CSI in terms of image quality (PSNR$_{TDI}$ = 42.3dB and PSNR$_{CSI}$ = 41.6dB). This is mainly because CSI uses a fraction of the available bandwidth. However, when tested both on the same bandwidth-limited data, CSI outperforms TDI as TDI suffers, for the presented example, from problems related to cycle-skipping. Meanwhile, TDI retrieves accurate reconstructions when using an unequal number of sources and receivers whereas CSI only works well when there are more receivers than sources. Also, using water as a starting model works equally well for both methods when there are sufficient sources and receivers. The reconstruction can be improved when a low-frequency model is used as starting model, specially in FDI when only a only 1 frequency is inverted. Finally, as compared to CSI, TDI requires a significant finer discretization of both time and space to avoid numerical dispersion or instability and as a consequence, TDI needs a larger amount of computing resources (15-80x) and memory requirements. To conclude, it is shown that TDI outperforms CSI in terms of image quality at the cost of a higher demand on computational resources.

References

[1] X. Ying, and Y. Lin, and X. Xia, and B. Hu, and Z. Zhu, and P. He, “A comparison of mammography and ultrasound in women with breast disease: a receiver operating characteristic analysis,” The Breast Journal, vol.18, no. 2, pp. 130–138, 2012.

[2] H. Gemmeke, and N.V. Ruiter, “3D ultrasound computer tomography for medical imaging,”, Nuclear Instruments and Methods in Physics Research Section A: Accelerators, Spectrometers, Detectors and Associated Equipment, Elsevier, vol. 580, no. 2, pp.1057–1065, 2007.

[3] A.B. Ramirez, and K.W.A. van Dongen, “Sparsity constrained Born inversion for breast cancer detection,” IEEE International Ultrasonics Symposium (IUS), (Taipei, Taiwan), 2015.

[4] N. Ozmen, and R. Dapp, and M. Zapf, and H. Gemmeke, Hartmut and N.V. Ruiter, and K.W.A. van Dongen, “Comparing different ultrasound imaging methods for breast cancer detection”, IEEE Transactions on Ultrasonics, Ferroelectrics, and Frequency Control, vol. 62, no. 4, pp. 637–646, 2015.

[5] G.Y. Sandhu, and C. Li, and O. Roy, and S. Schmidt, and N. Duric, “Frequency Domain Ultrasound Waveform Tomography: Breast Imaging Using a Ring Transducer,” Physics in Medicine and Biology, vol. 60, no. 14,pp. 5381-5398, 2015.

[6] O. Calderon, L. Guasch, P. Huthwaite, and M. Warner. “3D imaging of the breast using full-waveform inversion, International Workshop on Medical Ultrasound Tomography,” Speyer, Germany, 2017.

[7] A.B. Ramirez and K.W.A. van Dongen, “Sparsity Constrained Contrast Source Inversion,” Journal of Acoustical Society of America 140(3), 1749-1757, August 2016.

[8] J.F. Bakker, M.M. Paulides, I.-M. Obdeijn, G.C. van Rhoon and K.W.A. van Dongen, “An ultrasound cylindrical phased-array for deep heating in the breast: theoretical design using heterogeneous models,” Physics in Medicine and Biology 54, pp. 3201-3215, May 2009.